Drug Development and Industrial Pharmacy, 27(7), 719–729 (2001)

RESEARCH PAPER

Modeling of Powder Blending Using On-line Near-Infrared Measurements

Carlos Ufret* and Ken Morris†

Department of Industrial and Physical Pharmacy, Purdue University, West Lafayette, Indiana

ABSTRACT

A model to quantify the degree of mixing in pharmaceutical powder mixing operations was developed. The additive volume mixing model is based on the determination of the characteristic volume of agitation for a given blender, which is dependent on process parameters such as the formulation ingredients, the geometry of the mixer, and the batch load. The calculation of this characteristic volume of agitation is based on the determination of the fitted fraction of formulation mixed after the first blender rotation. A variation of this model, denominated the iterative mixing model, was also developed. On-line near-infrared (NIR) measurements were taken throughout the runs to obtain the mixing profile and the dynamics of the powder bed as a function of blender rotations. Studies were conducted at two scales using two different formulations to study and compare the calculated characteristic volume of agitation for each blender-formulation system. This approach elucidates the existing relationship between the characteristic mixing parameters and critical rotations (required rotations to achieve content uniformity) for a given system and represents a step toward scale-up of solids mixing operations.

INTRODUCTION

The first step in the manufacture of a quality dosage form is often the development of an efficient and reproducible solids mixing operation. This will yield a uniform distribution of components in the formulation or, in other words, a constant composition at every location within the mixture. The mixing profile for any given system is defined by diffusive, convective, and shear mechanisms that act

*Current address: Glaxo SmithKline Pharmaceuticals, P.O. Box 11975, Cidra, PR 00739-1975.
†Corresponding author.

simultaneously within the solids bed (1). Depending on the interparticle forces (e.g., molecular, electrostatic, gravitational) to which the particles are subjected and the type of mixing equipment used, any of these mechanisms may predominantly influence the mixing behavior of the system (2). Studies comparing the effectiveness of different types of mixers have been reported by several researchers (3).

Batch homogeneity may be a critical parameter to monitor to guarantee reproducibility of the properties of the manufactured dosage form at any production scale and to ensure compliance to given product specifications. Although mixing seems to be a straightforward operation, no definite and robust approach has been established to describe quantitatively the process dynamics. The complexity of this unit operation arises from the fact that multiple variables may influence the behavior of a powder bed undergoing rotational movement. These variables may be classified in two categories: "internal" parameters (particle shape, size distribution, moisture content, flowability, compressibility, etc.), which are characteristic of the formulation, and "external" parameters (type of mixer, mixer geometry, rotational speed, etc.), which describe the mixing equipment in which the operation takes place. The existing correlation between internal parameters such as moisture content, flowability, and compressibility was studied by Malhotra and Mujumdar (4).

In recent years, several researchers have suggested various approaches to assess batch homogeneity. Statistical methods based on mixing indices and analyses of variance (ANOVA) have been applied for binary and multicomponent systems, according to ordered or random mixing system characteristics (5,6). Stochastic approaches using Markov chain models and random walk numerical simulations based on probability have also been described (7). In-silo blending studies and residence time distribution (RTD) theories applied to flow patterns of solids in hoppers and bins have also aided in the understanding of flow dynamics in an enclosed system (8,9).

Fractal geometry concepts (10) and Monte Carlo methods have been applied to support the cascade (or avalanche) mixing hypothesis, which qualitatively describes the flow of particles inside a rotating drum (11,12). Cascading takes place at the surface of the powder bed, and granules flow downhill in the direction of rotation as a function of mixing intensity, while particles below the shear layer rotate with the mixer as a solid body (13). These chaotic dynamics result in a stick-slip motion of the shear layer below the cascading region, which causes the interface to increase exponentially (11). This physical behavior explains the first-order exponential mixing profile suggested by Train (14):

$$y = A(1 - e^{-kt}) \tag{1}$$

where y is the degree of mixing, A is the initial resistance of the powder, k is the rate of fine powder dispersion, and t is the mixing time. The value of the rate of fine powder dispersion determines how much time it takes for the mixing curve to reach the plateau value A.

Recently, discrete element modeling (DEM) has been utilized in mixing applications and granular flow studies (15–17). This technique is based on the determination of the magnitude of normal and tangential forces present at the contacts between individual particles during mixing, with elastic, dissipative, frictional, rotational, and translational force components balanced in order to predict the granular displacement profiles. Particle deformation mechanisms described by Young's modulus (18) and interparticle frictional forces are mainly responsible for the flow and mixing characteristics of the powder bed. Granular flow patterns are simulated by equations of motion, force algorithms, and the mechanical properties of the formulation components.

When applying any of these batch homogeneity assessment methods, it is important to be able to correlate the process parameters obtained from laboratory experiments to those at the production scale. For scale-up purposes, the main variables to consider are the mixer geometry (constant ratio of linear dimensions), process kinematics (equal ratio of velocities), and system dynamics (equal ratio of forces between corresponding points in the different mixers) (19). The Froude, Power, and Reynolds dimensionless coefficients have been used by many researchers in mixer scale-up applications (20,21).

At the production scale, sampling is conducted by means of a thief probe. However, inevitable bed disturbance and segregation of noncohesive material during thief cavity flow (22) have led to the development of new sampling methods. On-line process measurements have been investigated and applied to assess homogeneity continuously throughout a blending run without the need of interrupting the opera-

tion. Near-infrared (NIR) measurements have been used as a valuable technique to determine the degree of mixing and to represent a viable alternative to thief sampling in the near future (23–25).

This study presents a mathematical model to describe quantitatively the dynamics at the flowing region inside a mixer as it is rotated. This method is based on continuous on-line NIR measurement of uniformity, applied mathematics, and statistical regression analysis, as discussed in the following sections.

EXPERIMENTAL

Physical Description and Derivation of the Mathematical Model

The additive volume mixing model is based on the determination of the characteristic volume of agitation for a given blender, which represents the spatial region within the powder bed where exchange of material and particle rearrangement occurs as the blender is rotated. The dynamic behavior of the formulation in this characteristic region is representative of the entire mixing process. According to the proposed model, the volume of formulation mixed as a function of blender rotations is

$$V_r^{mix} = rV^o - \alpha \sum V_{r-1}^{mix} \tag{2}$$

where V^o is the characteristic volume of agitation, $\alpha \sum V_{r-1}^{mix}$ represents the cumulative volume of material remixed, and r is the number of blender rotations. The carryover volume α represents the fraction of material mixed in a specific rotation that remains in the characteristic region and is remixed at the following rotation. Equation 2 may also be expressed in units of fraction mixed:

$$f_r^{mix} = rf^o - \alpha \sum f_{r-1}^{mix} \tag{3}$$

After the first rotation, the cumulative remixing term $\alpha \sum f_{r-1}^{mix}$ is zero; in other words, for $r = 1$, it is observed that $f_r^{mix} = f^o$. Therefore, the characteristic fraction of mixing for a given blender is equivalent to the fraction of material mixed after the first rotation. Experimental determination of this parameter is assessed using NIR spectroscopy and statistical analysis.

The importance of the cumulative remixing term resides in that it physically distinguishes between what would be an ideal linear mixing profile (when no accumulation of material at the characteristic region exists) and the actual mixing profile observed. For an ideal system, a "steady-state" flowing region would exist where all unmixed powder that enters the blender's characteristic region at a given rotation is displaced at the end of the rotation by incoming material and so on until all the formulation has been mixed. This behavior yields a linear relationship between the total fraction of powder mixed and the number of mixer rotations. However, in real mixing operations, only a fraction of material mixed at a given rotation is displaced from the characteristic region of agitation. The remaining fraction of material is remixed in the subsequent rotation, and this pattern is repeated throughout the entire mixing run, yielding an exponential mixing profile (Fig. 1). After any given number of rotations, the summation of the differences between the ideal and actual fractions mixed in previous rotations corresponds to the cumulative amount of material remixed.

At any given rotation, the total volume of material inside the characteristic region consists of a fraction of formulation mixed for the first time and another fraction already mixed at a previous rotation. The fraction of powder mixed for the first time at a given rotation is represented by the difference between consecutive data points for the fraction mixed:

$$f_r^{m@r_i} = f_r^{mix} - f_{r-1}^{mix} \tag{4}$$

The fraction of powder remixed at a given rotation is

$$f_r^{remix@r_i} = \left(f_r^{mix,\,ideal@r_i} - f_r^{mix,\,actual@r_i}\right) - f_{r-1}^{remix@r_{i-1}} \tag{5}$$

where the actual fraction mixed $f_r^{mix,\,actual@r_i}$ is determined from Eq. 1, and the ideal fraction mixed is given by

$$f_r^{mix,\,ideal@r_i} = rf^o \tag{6}$$

Since these quantities are derived from the overall exponential mixing profile for the system, they are related exponentially to mixing time as well. The powder mixed for the first time at every rotation will decrease until it asymptotically approaches zero, while the powder being remixed will increase until it plateaus at a value equivalent to the characteristic fraction of the blender. At

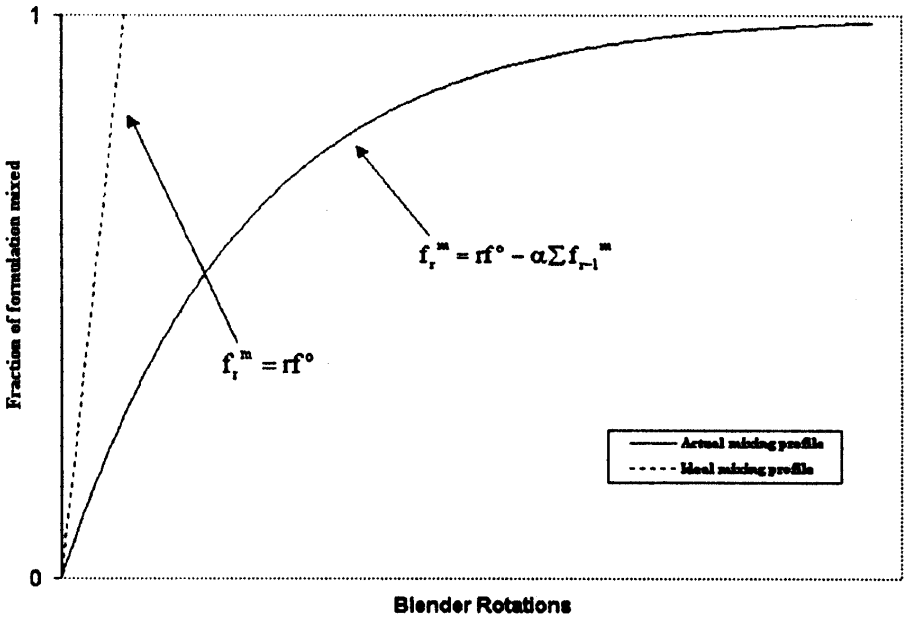

Figure 1. The theoretical exponential mixing profile of the fraction of material mixed versus the number of blender rotations: additive volume mixing model.

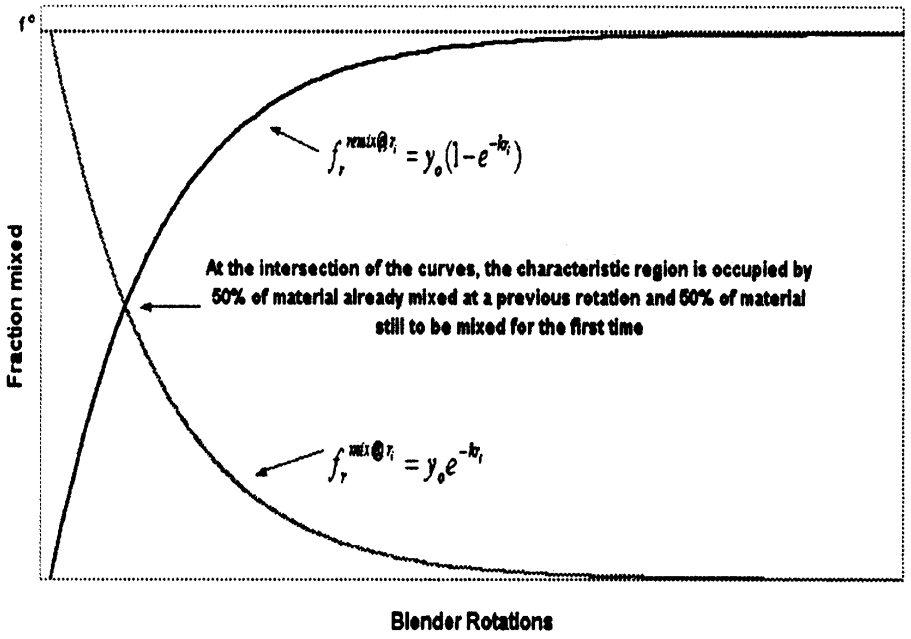

Figure 2. Theoretic exponential growth and decay mixing profiles within the characteristic region: additive volume mixing model.

this point, the formulation is considered to be homogeneous. This behavior is shown in Fig. 2. It may be seen that the sum of the two curves is equivalent to the characteristic fraction of mixing f^o at every rotation. The y-intercept of the remixing curve y_o has no physical meaning; it is merely a modeling parameter to describe the remixing curve.

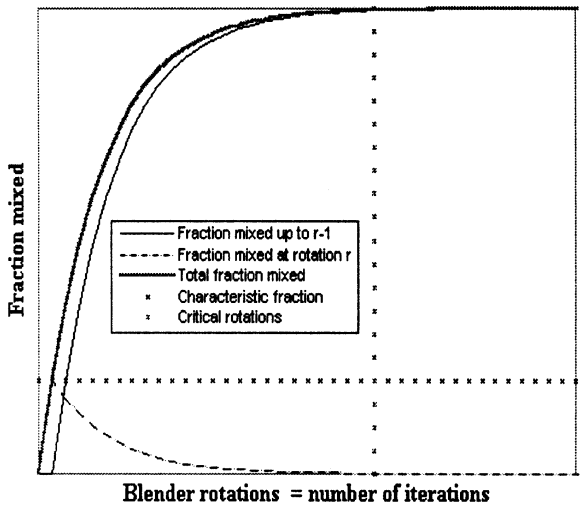

Figure 3. The theoretic mixing profile of the fraction of material mixed versus the number of blender rotations: iterative mixing model.

The calculated characteristic volume (or fraction) of agitation may be used as a basis to predict the critical rotations (required rotations to achieve content uniformity) at different loads of the mixing equipment. From Fig. 2,

$$f_r^{mix@r_i} = y_o e^{-kr_i} \tag{7}$$

From the definition of the characteristic fraction of mixing, at $r = 1$,

$$f^o = y_o e^{-k} \tag{8}$$

Rearranging Eq. 8,

$$y_o = f^o e^k \tag{9}$$

Since the mixing curve approaches zero asymptotically, the formulation may be considered homogeneous when the curve decreases to $0.02y_0$, designated as $y_{\min}$. Combining Eqs. 7 and 9, the value of r as $y \to 0$ is

$$r_{\text{crit}} = \frac{\ln(y_{\min}/y_0)}{-k} \cong -\frac{1}{k}\ln\left(\frac{y_{\min}}{f^o e^k}\right) \tag{10}$$

which for $0.06 \leq k \leq 0.10$ may be approximated:

$$r_{\text{crit}} \cong -\frac{1}{k}\ln\left[\frac{y_{\min}(1-k)}{f^o}\right] \tag{11}$$

Based on the discussed additive model, a modified approach based on iterative calculations was also developed. It is more practical than the additive volume mixing model because it only depends on the characteristic fraction (or volume) of agitation for a given system. The carryover volume term α is implicit in Eq. 12:

$$f_r^m = \sum f_{r-1}^m + f^o\left(1 - \sum f_{r-1}^m\right) \tag{12}$$

According to this expression, the fraction mixed up to a given rotation is the sum of the cumulative fraction mixed up to the previous rotation and the fraction mixed at the r rotation, which is a percentage of the still-unmixed formulation. Figure 3 graphically shows the mixing profile based on the iterative mixing model for a formulation in a rotating blender. As noted below, to apply the iterative model, there is no need to normalize the data, which represents an advantage over the additive model discussed above.

A more descriptive explanation of these two mathematical models is presented in the Appendix.

Procedure for the Development of the Additive Volume Mixing Model

1. Collect on-line spectroscopic data during blending runs.
2. Normalize NIR data to units of fraction mixed.
3. For the normalized NIR data sets, (a) plot normalized data as a function of rotations (or time); (b) smooth using moving averages (*MovAve*) or moving averages smoothing (*ExpSmo*); (c) run regression fit of smoothed data; determine the values of A and k (from Eq. 1).
4. Calculate (a) characteristic fraction f^o (fitted fraction mixed after first rotation); (b) fraction mixed for the first time at every rotation $f_r^{mix} - \sum f_{r-1}^{mix}$; (c) cumulative fraction of material remixed $\alpha \sum f_{r-1}^{mix}$.

Procedure for the Development of the Iterative Mixing Model

1. Collect on-line NIR data during blending runs and plot as a function of rotations (or time).
2. Determine r_{crit} directly from the mixing curve plateau.
3. Apply Eq. 12; by trial and error, determine the characteristic fraction required to reach unity after n iterations (where $n = r_{\text{crit}}$).

Near-Infrared Instrumentation and Statistical Analysis Package

Spectroscopic data were collected using the MM55 absorption gauge (manufactured by NDC Infrared Engineering, Irwindale, CA). The NIR instrument works on the principle of diffuse reflectance. The sensor measures changes in reflected intensity at areas of absorption of the powder bed and converts the information to the desired measurement through mathematical algorithms in the electronic control unit of the instrument (24). The instrument was focused toward a glass window located at the side of the blender, where it measured the ratio of incident and transmitted radiation, resulting in a signal logarithmically related to moisture content. TableCurve 2D software (SPSS Software, Chicago, IL) was used to perform the statistical analysis of the spectroscopic data and to run the regression fits.

Blending studies were conducted at two scales. Data were collected for each run and plotted as a function of blender rotations (or mixing time). The data were normalized to units of fraction mixed and smoothed using moving averages (*MovAve*) with a period of 2 min or exponential smoothing (*ExpSmo*). The values of A and k for first-order mixing were determined from least-squares regression fitting of the NIR data.

Materials and Methods

Small-Scale Study

The small-scale mixing experiments were carried out in a 1.5-ft^3 bin blender rotated at approximately 10 rpm. Four 8-kg formulations were prepared, consisting of a 3 : 1 mixture (w/w) of anhydrous lactose (Sheffield Products) and dibasic calcium phosphate dihydrate (DI-TAB) (Rhône-Poulenc) with 0.5% Cab-O-Sil® (Cabot Corp.) as a glidant to improve flow properties. Also, three 9-kg formulations consisting of a 5 : 1 mixture (w/w) of anhydrous lactose and active dihydrate with 0.5% Cab-O-Sil were prepared. All materials were passed through a 40-mesh screen and weighed on a Mettler P3 balance prior to blending. Data were collected after every blender rotation, with increasing intervals as the blending run progressed.

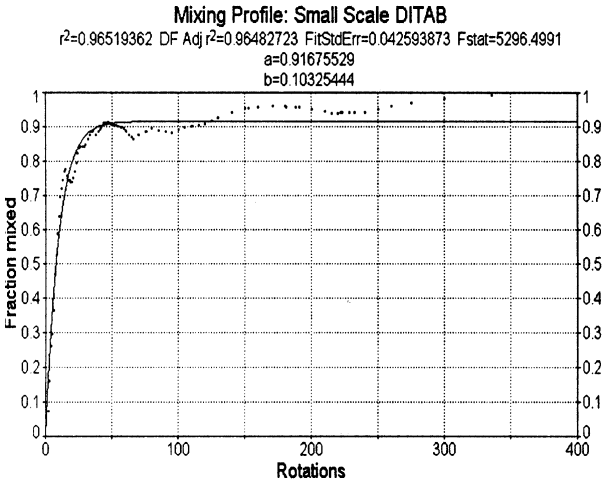

Figure 4. Small-scale blender DI-TAB mixing profile.

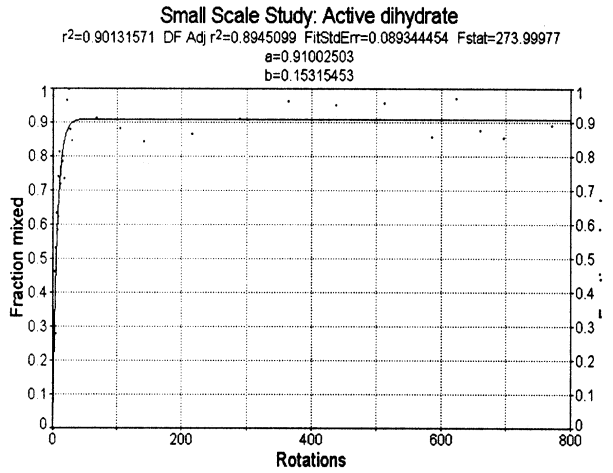

Figure 5. Small-scale blender active dihydrate mixing profile.

Large-Scale Study

Four runs were carried out in a 14.8-ft^3 bin blender, the first two consisting of 178 kg (140 kg anhydrous lactose, 20 kg active dihydrate, 18 kg A-TAB), the third consisting of 198 kg of formulation (160 kg anhydrous lactose, 20 kg active dihydrate, 18 kg A-TAB), and the fourth consisting of 200 kg of formulation (105 kg anhydrous lactose, 50 kg DI-TAB, 45 kg discharge from run 2). Magnesium stearate (0.3% w/w) was added to all formulations as a lubricant. The blender was rotated at 6 rpm. Spectroscopic data were collected continuously every 0.5 s until steady-state conditions were reached.

RESULTS AND DISCUSSION

Spectroscopic data was refined using *ExpSmo* and *MovAve*. Since *ExpSmo* gives less weight to past data as it is farther from the reference data point, it is more sensitive to outliers and to unexpected variations in trends. *MovAve* gives the same weight to all the values within a specified range from the reference point, so it is expected to provide smoother regression fits and higher correlation coefficients than *ExpSmo*. *MovAve* smoothing is valid when data are collected at regular time intervals, which was the case for the large-scale study. However, since spectroscopic data for the small-scale study were collected at irregular time intervals, locally weighted exponential smoothing (*LOESS*) was applied instead of *MovAve* (26,27). Normalization of the smoothed data yielded curves that exponentially grew from the origin to a plateau value of one.

For the DI-TAB small-scale study, all four runs were identical (8 kg consisting of 75% lactose anhydrous, 25% DI-TAB by weight). Figure 4 shows the mixing profiles when pooling the small-scale DI-TAB runs. For the active dihydrate small-scale study, the three runs were averaged, and the mean values were plotted as a function of rotations (see Fig. 5). The difference in the calculated characteristic fraction between the DI-TAB and the active dihydrate batches evidences the dependence of mixing behavior on the properties of the formulation.

Three large-scale active dihydrate runs were conducted. For run 2, an unexpected plateau was

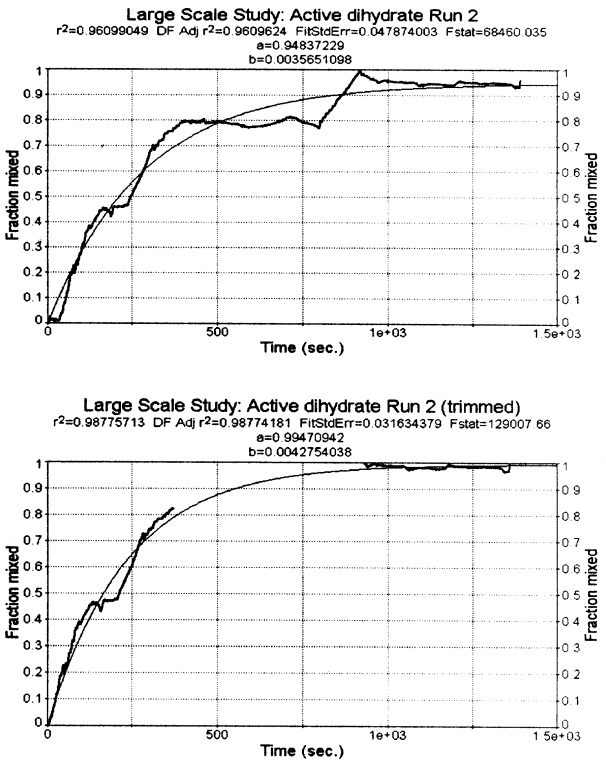

Figure 6. Large-scale blender active dihydrate run 2 mixing profile: (a) original data; (b) after trimming.

Table 1

Results for Individual Large-Scale Active Dihydrate Runs

Run	Characteristic		
	Fraction (F^o)	Mass (kg)	Critical Rotations r_{crit}
1	3.95%	7.11	97
2	3.50%	6.30	110
2[a]	4.19%	7.54	92
3	4.53%	9.06	84

[a]Trimmed.

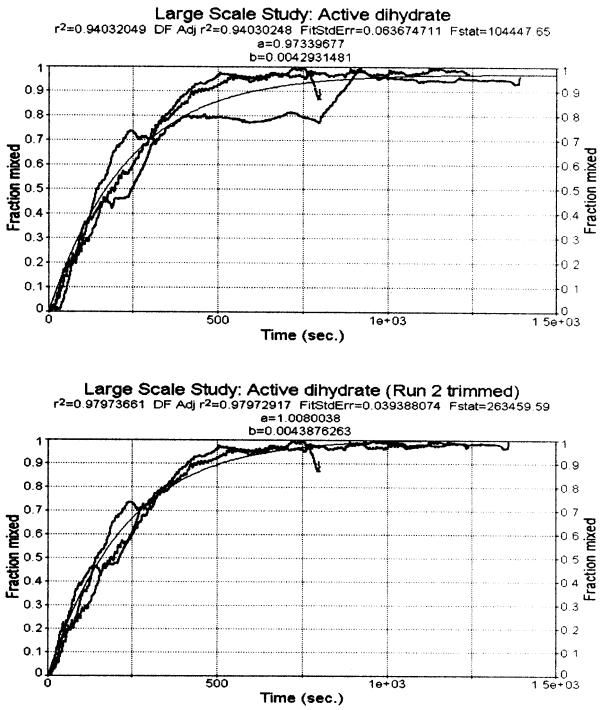

Figure 7. Pooled large-scale blender active dihydrate mixing profile: (a) original data; (b) after trimming.

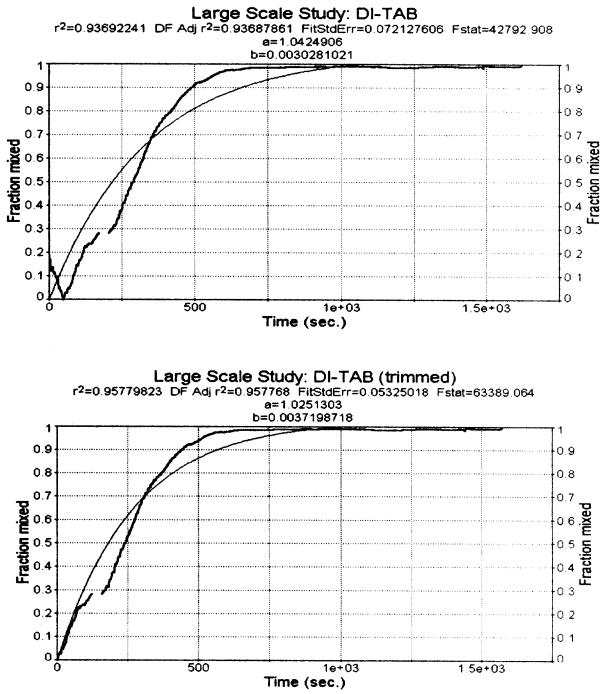

Figure 8. Large-scale blender DI-TAB mixing profile: (a) original data; (b) after trimming.

Table 2

Calculated Characteristic Fractions and Scale-up Coefficients

Formulation	Small Scale (%)	Large Scale (%)	Scale-up Coefficient $S_{\text{characteristic}}$
DI-TAB	9.81	2.98	3.29
DI-TAB[a]		3.65	2.69
Active dihydrate	14.20	4.20	3.38
Active dihydrate[b]		4.30	3.30

[a]After trimming data.
[b]After trimming run 2.

observed between 400 and 800 s (see Fig. 6a), so the corresponding data was trimmed to assess the effect of this deviation on the calculated characteristic parameters for the system (see Fig. 6b). Table 1 shows the calculated characteristic parameters and critical rotations for the individual runs. The original and trimmed sets of data were incorporated to the pooled mixing profiles as shown in Fig. 7; the overall mixing behavior for the large-scale active dihydrate system is best described by Fig. 7b instead of Fig. 7a since the apparent plateau in run 2 (from 400 to 800 s) is not representative of the mixing process.

An unexpected trend was also observed for the large-scale DI-TAB study; a decreasing profile was seen during the first 500 s (see Fig. 8a), which obviously influenced the calculations. Figure 8b shows the mixing profile after trimming the suspect data; as expected, the characteristic fraction increased considerably.

Table 2 shows the calculated characteristic fraction for each formulation and scale, including the cases for which data were trimmed. A *characteristic* scale-up coefficient $S_{\text{characteristic}}$, defined as the ratio of characteristic fractions for a given formula at two scales, was calculated for both formulations. A *critical* scale-up coefficient S_{crit} based on the ratio of critical rotations yielded the same results, which is expected due to the existing relationship between characteristic fraction and critical rotations (see Table 3). Slight differences between the two scale-up coefficients were observed as a result of rounding numbers. From the S values, it may be inferred that the characteristic fraction for a given system is influenced by process scale, among other variables.

Several factors could have influenced the calculation of the characteristic parameters and scale-up coefficients. First, the ratios of excipients in the large- and small-scale studies, although close, were not identical. It is known that critical mixing parameters such as flowability and particle packing are influenced by the formulation properties. Second, the flowing region is influenced by the blender geometry; that is, the width of the blender at the bed surface determines the lateral displacement of the flowing material as the blender is rotated. The geometries of the large- and small-scale blenders were not identical. Third, as observed from Figs. 6 and 8, unexpected trends in the mixing profiles may considerably influence the characteristic parameters of a system. For our study, the NIR data were validated by simultaneously collecting samples with a thief probe and comparing it to on-line measurements. The same trends were observed after off-line analysis of the collected samples, which shows that the suspect data were "process related" and independent of the sampling technique used.

Another justification for the high characteristic fractions obtained for the small blender study is the

Table 3

Critical Rotations for Every Blender-Formulation Combination

Formulation	Small Scale (%)	Critical Rotations r_{crita}	Large Scale (%)	Critical Rotations r_{crit} [a]	Scale-up Coefficient S_{crit}
DI-TAB	9.81	39	2.98	130	3.33
DI-TAB[b]			3.65	106	2.72
Active dihydrate	14.20	27	4.20	92	3.41
Active dihydrate[c]			4.30	90	3.33

[a]To nearest rotation.
[b]After trimming data.
[c]After trimming run 2.

fact that the blender was stopped after every rotation to collect the spectroscopic data. This interruption resulted in additional turbulence of the powder bed, which enhances flow perturbations and increases mixing intensity. It has been shown by several researchers that rocking mechanisms in a rotating blender at the laboratory scale may increase the rate of mixing when compared to a conventional blender (31,32). Although the rocking motion in the small-scale study was unintended and only present at a slight level compared to the aforementioned experiments, it may have influenced the calculations. Since the spectroscopic data for the large-scale blender were collected continuously, no significant external rocking mechanisms were considered.

Although the conditions and process variables were not identical throughout the study, the proposed mixing models and the concept of a characteristic volume of agitation for a given formulation-scale system represent a suitable approach for scale-up studies of powder mixing operations based on this study.

CONCLUSIONS

The additive volume mixing model and the subsequently derived iterative mixing model were developed to describe quantitatively the mixing behavior of a pharmaceutical formulation inside a bin blender as it is rotated. The model is based on the determination of the characteristic fraction of mixing for a given blender, which may be subsequently converted to units of volume or mass to quantify the flow of material at every rotation. Two related models were proposed for the calculation of the characteristic volume of agitation; the first is based on fitting on-line near-infrared measurements to the theoretical first-order mixing model; the second is based on direct visualization of the mixing curve plateau and iterative calculations. The dynamics of the flowing particles within the characteristic region of the powder bed were derived mathematically from the mixing profile. The calculation of scale-up coefficients quantitatively evidenced the influence of formulation properties, mixer geometry, and process scale on the mixing behavior of a system.

APPENDIX

Supplementary Analysis

The following mathematical analysis provides a brief quantitative description of the relationship between the modeling parameters described in the Experimental section. From Eq. 3, the fraction of material mixed is

$$f_r^{mix} = rf^o - \alpha \sum f_{r-1}^{mix}$$

Dividing the expression by the cumulative mixing term $\alpha \sum f_{r-1}^{mix}$,

$$\frac{f_r^{mix}}{\alpha \sum f_{r-1}^{mix}} = \left(\frac{r}{\alpha \sum f_{r-1}^{mix}}\right) f^o - 1$$

It may be observed that a linear relationship exists between the term on the left side of the equation and the term in parentheses on the right side of the equation. The straight line will have a slope equivalent to the characteristic fraction mixed f^o and a y-intercept equal to -1. All the parameters shown in the equation were calculated using Eqs. 4 through 7.

Since the fraction mixed after the first rotation is equivalent to the characteristic fraction mixed, at the second rotation, $\sum f_{r-1}^{mix} = f^{\circ}$. Therefore, we may easily determine the carryover fraction from the mixing data at the second rotation:

$$f_{r=2}^{mix} = rf^{o} - \alpha \sum f_{r-1}^{mix} = rf^{o} - \alpha f^{\circ}$$

For example, solving for α (at $r = 2$), we obtain an expression for the carryover fraction based only on the first two data points of the mixing profile:

$$\alpha = 2 - \left(\frac{f_{r=2}^{mix}}{f^{\circ}}\right) \tag{14}$$

After the second rotation, the value of $\alpha_r - \alpha_{r-1}$ will gradually increase until it approaches $\alpha_{r=2}$. The number of rotations it takes to reach this value is equivalent to the critical rotations r_{crit}.

For the iterative mixing model, the characteristic fraction of agitation for a system is determined graphically from the mixing curve without the need of determining the powder dispersion rate k, which makes it more practical than the additive volume mixing model. The critical rotations for a given system are read directly from the plateau of the mixing curve and are equivalent to the number of iterations required to reach $f_{rm} = 1$ (mixing degree = 100%). The conditions for complete mixing are numerically described using Eq. 15:

$$\sum_{1}^{r_{crit}} f_r^m \cong \sum_{1}^{r_{crit}} f_{r-1}^m \cong 1 \tag{15}$$

After the first rotation, $\sum f_{r-1}^{m} = 0$; after the second rotation, $\sum f_{r-1m} = f^{o}$, and so on until $\sum f_{r-1m} = f_{rm}$, where the curve approaches unity, and the batch is completely mixed.

NOMENCLATURE

α	carryover volume
A	initial resistance of the powder
$ExpSmo$	exponential smoothing
f^{o}	characteristic fraction of mixing
f_r^{mix}	fraction of material mixed
$f_r^{mix@r}$	fraction of material mixed for the first time at a given rotation r
$f_r^{remix@r}$	fraction of material re-mixed at a given rotation r
$f_r^{mix,\,ideal@r}$	ideal fraction of material mixed at a given rotation r
k	rate of fine powder dispersion
$MovAve$	moving averages smoothing
m^{o}	characteristic mass of agitation
r	rotations
r_{crit}	critical rotations
t	time
S	scale-up coefficient
$S_{\text{characteristic}}$	scale-up coefficient calculated from characteristic fraction
S_{crit}	scale-up coefficient calculated from critical rotations
V	volume mixed
V^{o}	characteristic volume of agitation
y	degree of mixing
y_o	y-intercept of characteristic region exponential decay mixing profile
$\sum f_{r-1}^{mix}$	total fraction of material mixed at a previous rotation
$\sum V_{r-1}^{mix}$	total volume of material mixed at previous rotation

ACKNOWLEDGMENT

We wish to acknowledge gratefully the support of the Consortium for the Advanced Manufacturing of Pharmaceuticals (CAMP) at Purdue University and Ravi Menon, Gary Van Savage, and Francois Menard of Johnson and Johnson, OMP.

REFERENCES

1. Poux, M.; Fayolle, P.; Bertrand, J.; Bridoux, D.; and Bousquet, J. Powder mixing: some practical rules applied to agitated systems. Powder Technol. **1991**, *68*, 213–234.
2. Fan, L.T.; Chen, Y.; and Lai, F.S. Recent developments in solids mixing. Powder Technol. **1990**, *61*, 255–287.
3. Palmieri, G.F.; Lovato, D.; Marchitto, L.; Zanchetta, A.; Martelli, S. Evaluation of the mixing effectiveness of a new powder mixer. Drug Dev. Ind. Pharm. **1998**, *24* (1), 81–88.
4. Malhotra, K.; Mujumdar, A.S. Particle mixing and solids flowability in granular beds stirred by paddle-type blades. Powder Technol. **1990**, 61, 155–164.
5. Walker, J.J.; Rollins, D.K. Detecting powder mixture inhomogeneity for non-normal measurement errors. Powder Technol. **1997**, *92*, 9–15.
6. Schmidli, H.; Grize, Y.L. Quantification of batch homogeneity. Qual. Eng. **1997–1998**, *10* (2), 359–364.

7. Das Gupta, S.; Khakhar, D.V.; Bhatia, S.K. Axial transport of granular solids in horizontal rotating cylinders. Part 1: Theory. Powder Technol. **1991**, *67*, 145–151.
8. Cassidy, D.J.; Scrivens, B.G.; Michaelides, E.E. An experimental study of the blending of granular materials. Powder Technol. **1992**, *72*, 177–182.
9. Standish, N.; Lui, Y.N.; McLean, A.G. Quantification of the degree of mixing in bins. Powder Technol. **1988**, *54*, 197–208.
10. Kaye, B.H. Characterizing the flowability of a powder using the concepts of fractal geometry and chaos theory. Part. Syst. Charact. **1997**, *14*, 53–66.
11. Shinbrot, T.; Alexander, A.; Muzzio, F.J. Spontaneous chaotic granular mixing. Nature **1999**, *397*, 675–678.
12. Metcalfe, G.; Shinbrot, T.; McCarthy, J.J.; Ottino, J.M. Avalanche mixing of granular solids. Nature **1995**, *374*, 39–41.
13. Campbell, H.; Bauer, W.C. Cause and cure of demixing in solid-solid mixers. Chem. Eng. **1966**, 179–185.
14. Train, D.J. J. Am. Pharm. Assoc., Sci. Ed., 49: 265 (1960).
15. Mugurama, Y.; Tanaka, T.; Kawatake, S.; Tsuji, Y. Discrete particle simulation of a rotary vessel mixer with baffles. Powder Technol. **1997**, *93*, 261–266.
16. Jensen, R.P.; Bosscher, P.J.; Plesha, M.E.; Edil, T.B. DEM simulation of granular media–structure interface: effects of surface roughness and particle shape. Int. J. Num. Anal. Meth. Geomech. **1999**, *23*, 531–547.
17. Cleary, P.W.; Metcalfe, G.; Liffman, K. How well do discrete element granular flow models capture the essentials of mixing processes? Appl. Math. Modelling **1998**, *22*, 995–1008.
18. Bassam, F.; York, P.; Rowe, R.C.; Roberts, R.J. The Young's modulus of binary powder mixtures. Powder Technol. **1991**, *65*, 103–111.
19. Van der Waat, J.G.; de Villiers, M.M. The effect of V-mixer scale-up on the mixing of magnesium stearate with direct compression microcrystalline cellulose. Eur. J. Pharm. Biopharm. **1997**, *43*, 91–94.
20. Landín, M.; York, P.; Cliff, M.J.; Rowe, R.C. Scaleup of a pharmaceutical granulation in planetary mixers. Pharm. Dev. Technol. **1999**, *4* (2), 145–150 (1999).
21. Horsthuis, G.J.B.; van Laarhoven, J.A.H.; van Rooij, R.C.B.M.; Vromans, H. Studies on upscaling parameters of the Gral high shear granulation process. Int. J. Pharm. **1993**, *92*, 143–150.
22. Carstensen, J.T.; Dali, M.V. Blending validation and content uniformity of low-content, noncohesive powder blends. Drug Dev. Ind. Pharm. **1996**, *22* (4), 295–290.
23. Sekulic, S.S.; Wakeman, J.; Doherty, P.; Hailey, P.A. Automated system for the on-line monitoring of powder blending processes using near-infrared spectroscopy Part II. Qualitative approaches to blend evaluation. J. Pharm. Biomed. Anal. **1998**, *17*, 1285–1309.
24. Han, S.M. Direct moisture during granulation using a near-infrared filter instrument. Paper presented at the 1996 Annual Meeting of the American Association of Pharmaceutical Scientists, Seattle, 1998.
25. Wargo, D.J.; Drennen, J.K. Near-infrared spectroscopic characterization of pharmaceutical powder blends. J. Pharm. Biomed. Anal. **1996**, *14*, 1415–1423.
26. Grznar, J.; Booth, D.E.; Sebastian, P. A robust smoothing approach to statistical process control. J. Chem. Inf. Comput. Sci. **1997**, *37* (2), 241–248.
27. Hitchman, P.A.; Berthouex, P.M. Exponential smoothing of monitoring data. J. Environ. Eng. **1986**, *112* (3), 551–564.
28. Lachman, L.; Lieberman, H.A.; Kanig, J.L. *The Theory and Practice of Industrial Pharmacy*, 3rd Ed.; Lea and Febiger: Philadelphia, 1986; 11–13.
29. Brone, D.; Alexander, A.; Muzzio, F.J. Quantitative characterization of mixing of dry powders in V-blenders. AICHE J. **1998**, *44* (2), 271–278.
30. Woodle, G.R.; Munro, J.M. Particle motion and mixing in a rotary kiln. Powder Technol. **1993**, *76*, 241–245.
31. Brone, D.; Wightman, C.; Connor, K.; Alexander, A.; Muzzio, F.J.; Robinson, P. Using flow perturbations to enhance mixing of dry powders. Powder Technol. **1997**, *91*, 165–172.
32. Wightman, C.; Mort, P.R.; Muzzio, F.J.; Riman, R.E.; Gleason, E.K. The structure of mixtures of particles generated by time-dependent flows. Powder Technol. **1995**, *84*, 231–240.